REPUBLIC OF TURKEY
ACIBADEM MEHMET ALİ AYDINLAR UNIVERSITY
INSTITUTE OF NATURAL AND APPLIED SCIENCES

DESIGN OF AN fNIRS BASED BCI SYSTEM FOR IDENTIFICATION OF IMPULSIVITY IN ADOLESCENTS

GÜLNAZ YÜKSELEN
MASTER'S THESIS

DEPARTMENT OF BIOMEDICAL ENGINEERING

SUPERVISOR
Assist. Prof. Sinem Burcu Erdoğan

İSTANBUL-2022

DECLARATION

I declare that the information reported in this thesis is the result of my own work, except where explicitly stated otherwise in the text. I am fully aware of all the ethical rules and there are not any violation of copyright and any kind of patent.

03.06.2022

Gülnaz Yükselen

ACKNOWLEDGEMENT

I am tremendously grateful to all the people who made this work possible, and I would like to mention some names in particular.

First of all, I would like to express my deepest appreciation to my supervisor Assist. Prof. Sinem Burcu Erdoğan, for the continuous support during this study. Her immense knowledge, enthusiasm, and guidance have continuously encouraged me in my academic research and daily life. Her invaluable patience and support helped me overcome many crises.

Furthermore, I would like to take this opportunity to express my gratitude to Prof. Ata Akın, Dean of the Faculty of Engineering, for his guidance, expertise, and significant discussions. I feel profoundly fortunate to have such a great and foresightful mentor.

Last but not least, I would like to thank my family. I am deeply grateful for their endless reliance and continuous encouragement. Their belief in me has kept my motivation high during this process. This work is dedicated to my adorable niece Bilge.

This study has been funded by Scientific and Technological Research Council of Turkey (TÜBİTAK-TEYDEB 1501) under Grant No. 3160652.

TABLE OF CONTENTS

LIST OF ABBREVIATIONS

ACC	Accuracy
ADHD	Attention Deficit and Hyperactivity Disorder
ALL	Combination of All Features of Clinical, Behavioral and Hemodynamic Datasets
ALL_{sf}	Combination of Selected Features of Clinical, Behavioral and Hemodynamic Datasets
ANN	Artificial Neural Networks
BCI	Brain-Computer Interface
BEH_{all}	All Features of Behavioral Domain
BEH_{sf}	Selected Features of Behavioral Domain
BPA	Back-Propagation Algorithm
C	Congruent Stimulus
CL_{all}	All Features of Clinical Domain
CL_{sf}	Selected Features of Clinical Domain
CQ	Cognitive Quotient
CQ_{IC-C}	Stroop Interference of Cognitive Quotient Metric (Incongruent-Congruent)
CQ_{IC-N}	Stroop Interference of Cognitive Quotient Metric (Incongruent-Neutral)
et al.	and others
FC	Functional Connectivity
fMRI	Functional Magnetic Resonance Imaging
fNIRS	Functional Near-Infrared Spectroscopy
GE	Global Efficiency
HbO	Oxygenated Hemoglobin
HbR	Deoxygenated Hemoglobin
HbT	Total Hemoglobin
$HEMO_{all}$	All Features of Hemodynamic Domain
$HEMO_{sf}$	Selected Features of Hemodynamic Domain

IC	Incongruent Stimulus
IMP	Impulsive Subjects
LED	Light Emitting Diode
ML	Machine Learning
MVPA	Multivariate Pattern Analysis
N	Neutral Stimulus
NE	Neural Efficiency
NE_{IC-C}	Stroop Interference of Neural Efficiency Metric (Incongruent-Congruent)
NE_{IC-N}	Stroop Interference of Neural Efficiency Metric (Incongruent-Neutral)
NEH	Neural Efficiency Hypothesis
NIC	Non-Impulsive Control Subjects
NIR	Near Infrared
OFC	Orbitofrontal Cortex
PC	Partial Correlation
PFC	Prefrontal Cortex
PUK	Pearson VII Kernel
RBF	Radial Basis Function
RT	Reaction Time
SCWT	Stroop Color and Word Test
SMO	Sequential Minimal Optimization
SVM	Support Vector Machines

LIST OF FIGURES

LIST OF TABLES

SUMMARY

Design of an fNIRS-based BCI System for Identification of Impulsivity in Adolescents

Currently, the diagnostic procedure for impulsivity is based on structured interviews, self-reports, and questionnaires which are highly subjective. This study aimed to develop a functional near-infrared spectroscopy (fNIRS) based decision-support system for identification of impulsivity in adolescents. Considering the multifaceted nature of impulsivity, it is proposed that feeding classification algorithms with multidomain features could better clarify the neurobiology underlying the symptoms of impulsivity. 38 patients (29 females, ages 15.6 ± 2.4) diagnosed with impulsivity and 33 non-impulsive control subjects (23 females, ages 15.1±1.9) participated in the study. Behavioral and hemodynamic metrics were collected during a Stroop task with concurrent fNIRS recordings. Functional connectivity (FC)-based features were calculated from the hemodynamic signals, and a neural efficiency metric was calculated by fusing the behavioral and FC-based features. The efficacy of two commonly used machine-learning (ML) algorithms, namely the support vector machines (SVM), and artificial neural networks (ANN) in classification of impulsive and control subjects was tested. A wrapper-based feature selection method was utilized to remove redundant features. Feature selection was employed for each domain individually, and 3 features from each domain were selected. Each classification algorithm was run 10 times with 10-fold cross-validation using combinations of the 3-domain feature set before and after employing feature selection. Both SVM and ANN achieved accuracies above 90% when trained with the combination of selected clinical, behavioral, and hemodynamic features. The SVM resulted in significantly higher accuracy than ANN (92.2% and 90.16%, respectively, p = 0.005). Preliminary findings show the feasibility of both ML-based methods for accurate identification of impulsivity when trained with multidomain features. The proposed classification approach has the potential to improve the clinical diagnosis of impulsivity and other psychiatric disorders. Our findings also pave the way for a computer-assisted diagnosis perspective on impulsivity severity rating.

Keywords: Brain-computer interface, Classification, Functional near-infrared spectroscopy, Impulsivity, Stroop test

ÖZET

Ergenlerde Dürtüselliğin Belirlenmesi İçin İYKAS Tabanlı Bir BBA Sistemi Tasarımı

Günümüzde, dürtüsellik için teşhis prosedürü, yapılandırılmış görüşmelere, kişisel raporlara ve oldukça öznel olan anketlere dayanmaktadır. Bu çalışma, ergenlerde dürtüselliğin tanımlanması için işlevsel yakın kızılaltı spektroskopi (İYKAS) tabanlı karar destek sistemi geliştirmeyi amaçlamaktadır. Dürtüselliğin çok yönlü doğası göz önüne alındığında, sınıflandırma algoritmalarını çok alanlı özelliklerle beslenmenin dürtüsellik semptomlarının altında yatan nörobiyolojiyi daha iyi aydınlatabileceği önerilmektedir. Çalışma, dürtüsellik tanısı konulmuş 38 hasta (29 kadın, yaşları 15,6 ± 2,4) ve dürtüsel olmayan 33 katılımcıdan (23 kadın, yaşları 15,1 ± 1,9) oluşan kontrol grubu ile gerçekleştirilmiştir. Bir Stroop görevi sırasında eşzamanlı İYKAS kayıtları ile davranışsal ve hemodinamik ölçümler toplanmıştır. Fonksiyonel bağlantı (FB) tabanlı özellikler hemodinamik sinyallerden hesaplanırken sinirsel verimlilik metriği, davranışsal ve FB tabanlı özelliklerin birleştirilmesiyle hesaplanmıştır. Yaygın olarak kullanılan iki makine öğrenmesi (MÖ) algoritmasının, destek vektör makineleri (DVM) ve yapay sinir ağları (YSA), dürtüsel ve kontrol grubu katılımcılarını sınıflandırmasındaki etkinliği test edilmiştir. Gereksiz özellikler sarmal tabanlı özellik seçimi kullanılarak ortadan kaldırılmıştır. Her alan için ayrı ayrı özellik seçimi yapılmış ve her alandan 3 özellik seçilmiştir. Her sınıflandırma algoritması, özellik seçiminin kullanılmasından önce ve sonra olmak üzere 3 alanlı özellik kümesi kombinasyonları kullanılarak 10 katmanlı çapraz doğrulama ile 10 kez çalıştırılmıştır. Hem DVM hem de YSA, seçilen klinik, davranışsal ve hemodinamik özelliklerin kombinasyonu ile eğitildiğinde % 90'ın üzerinde doğruluğa ulaşmıştır. DVM, YSA'dan istatistiksel olarak anlamlı ölçüde daha yüksek doğruluk sağlamıştır (sırasıyla %92,2 ve %90,16, p=0,005). Ön bulgular, çok alanlı özelliklerle eğitildiğinde dürtüselliğin doğru tanımlanması için her iki MÖ tabanlı yöntemin de uygulanabilirliğini göstermektedir. Önerilen sınıflandırma yaklaşımı, dürtüsellik ve diğer psikiyatrik bozuklukların klinik tanısını geliştirme potansiyeline sahiptir.

Bulgularımız ayrıca dürtüsellik şiddeti derecelendirmesi konusunda bilgisayar destekli bir teşhis perspektifinin önünü açmaktadır.

Anahtar Kelimeler: Beyin-bilgisayar arayüzü, Dürtüsellik, İşlevsel yakın kızılaltı spektroskopi, Sınıflandırma, Stroop testi

1. INTRODUCTION

Impulsivity is a multifaced neurodevelopmental disorder that has aspects associated with inadequate motor planning, lack of attention, and/or lack of forethought (1). As a characteristic trait, highly impulsive people typically struggle to implement cognitive control, which frequently results in actions that are poorly perceived, inappropriate to the situation, or commonly have negative future consequences (2).

In clinical practice, impulsivity is diagnosed by using structured interviews, self-reports such as the Barratt impulsiveness scale (3),questionnaires, and observational data. However, data obtained from conventional methods are highly subjective and frequently show variability across different methods. Such a discrepancy may occur due to the multifaceted nature of impulsivity in addition to its multifactorial etiology. Furthermore, the diagnostic procedure depends on the practical knowledge and experience of the clinician, which may also result in variability in diagnosis across different clinicians and cultures. Consequently, there is a demand for the availability of an objective and reliable system for accurate diagnosis.

Functional near-infrared spectroscopy (fNIRS) is a relatively novel, non-invasive, and wearable optical neuroimaging technology. By using near-infrared light, fNIRS measures the hemodynamic changes of the cerebral cortex (4,5). The main advantages of fNIRS are its low-cost and portable instrumentation, the ability to monitor hemodynamic activity in naturalistic settings, and overall ease of use (6). By transmitting light in the near-infrared spectral range (typically in 650-1000nm wavelength) through light emitting diodes (LED) placed on ergonomic probes, it has been shown that each light source is able to penetrate the scalp and measure temporal changes in the concentration of oxygenated hemoglobin (HbO) and deoxygenated hemoglobin (HbR) in probed brain tissue (7). fNIRS has demonstrated its ability to measure local hemodynamic changes induced during various cognitive and mental tasks (i.e., mental object rotation (8,9) that include motor imagination (10–12), and mental arithmetic operations (13–17).

Recent studies have explored the predictive value of various combinations of behavioral metrics and neuropsychological test measures for accurate distinction of children with attention-deficit and hyperactivity disorder (ADHD) from control subjects through the leverage of machine learning (ML) algorithms, (18–23). Alterations in functional activity and functional connectivity (FC) of the frontal brain regions were observed in children with ADHD when compared to age matched healthy control subjects (18–25) in both fNIRS (21–23) and functional magnetic resonance imaging (fMRI) studies (18,20,26). In addition to these studies, many neuroimaging studies have tested the utility of ML methods for classification of psychiatric disorders (27) and have demonstrated the promise of neuroimaging-based measures for objective diagnosis (26). However, to date, there have been no studies that focused on identification of impulsivity by using multivariate pattern analysis (MVPA) methods complemented with fNIRS-based neurophysiological features, behavioral and clinical metrics.

This study aimed to develop an fNIRS-based brain-computer interface (BCI) system that uses ML approaches to accurately identify impulsivity in adolescents. Considering the multifaceted nature of impulsivity in addition to its multifactorial etiology, it is proposed that combining informative features from clinical, behavioral, and hemodynamic domains may better clarify the neurobiology underlying the symptoms of impulsivity. With this motivation, behavioral and hemodynamic data were collected from 38 patients with high risk for impulsivity (IMP) and 33 non-impulsive control (NIC) subjects during a Stroop task with concurrent fNIRS recordings. A novel approach to the computation of FC-based metrics from hemodynamic signals acquired from the prefrontal cortex (PFC) was proposed, and a neural efficiency (NE) metric was computed by combining behavioral performance metrics during the Stroop test with the FC metrics. The efficacy of using multidomain feature sets in the classification of IMP and NIC subjects was tested by constructing classification models with two commonly used classifiers, namely support vector machines (SVM) and artificial neural networks (ANN).

The preliminary results demonstrate the feasibility of both algorithms for objective identification of impulsivity by using the selected features from different domains. Objectification of the diagnostic decision-making process of clinicians have been a critical issue. This study presents a solution approach to this critical problem with an fNIRS-based BCI system that integrates ML models with multidomain features obtained from behavioral, hemodynamic, and clinical domains. The efficacy of the proposed approach is demonstrated through a two class classification problem where the presence of impulsivity is predicted. No previous study has utilized fNIRS-driven novel FC metrics in the classification of IMP and NIC subjects using ML methods. Due to its significant accuracy performance, it is proposed that the reported ML-based classification approach may assist the clinician's diagnosis by providing a decision outcome.

2. BACKGROUND

2.1. Impulsivity

Various definitions of impulsivity exist in psychiatry literature. Impulsivity has been separated into three components by Patton et al. (1995), i) “an inability to focus attention or concentrate” (attentional impulsiveness), ii) “as acting without thinking”, (motor impulsiveness), and iii) “lack of forethought” (non-planning impulsiveness) (3). Eysenck (1977), associated impulsivity with risk-taking, inability to plan, and lack of concentration (28). In the experimental-behavioral sense, impulsivity is defined as selecting very small but direct rewards instead of large and delayed rewards (29). Impulsivity can also be defined as an untimely expressed and risky pervasive action which often leads to undesirable consequences and inappropriate situations.

The PFC and orbitofrontal cortex (OFC) are involved in the control of suppression, decision making, and response selection processes. The OFC plays an important role in guiding behavior based on available knowledge about the consequences of one's actions. Therefore, impulsivity is frequently observed in people with frontal lobe damage.

2.2. The Stroop Color and Word Test

The Stroop Color and Word Test (SCWT) is a widely used neuropsychological test for both clinical and experimental purposes. The SCWT has been used as a classic measure of frontal lobe function since its introduction in 1935 (30). In this task, the subject is instructed to name the ink color instead of reading the text (i.e., ‘BLUE’ printed in yellow ink). Since word reading is a more automated task than color naming, subjects must overcome cognitive interference and inhibit the incorrect, but more straightforward, response to respond correctly (31,32). The difficulty in the inhibition of performing a more automated task is recognized as the Stroop effect (30). Although the SCWT is commonly used to measure the ability to inhibit cognitive interference, it has also been used to assess other cognitive functions including processing speed, attention, cognitive flexibility (33), and working memory (34). Hence, the SCWT can be used to measure multiple cognitive functions. Numerous studies in the neuroimaging literature have employed the SCWT to measure inhibitory cognitive control and investigate neural correlations of cognitive interference effect in healthy subjects. Activations in prefrontal and cingulate cortical regions during Stroop interference have been shown coherently in neuroimaging studies (35,36).

2.3. Functional Near Infrared Spectroscopy

fNIRS is a non-invasive, wearable optical neuroimaging technology that measures the concentration changes of HbO and HbR in brain tissue in response to neuronal activation. By utilizing the relative transparency of the biological tissue within this near infrared (NIR) optical window, NIR light shining into the head (typically in the wavelength range of 650-1000 nm) will reach the brain tissue.

The discovery of fNIRS dates back to 1977 (7). Fransis Jobsis observed that red light was capable of penetrating a 4-mm thick beefsteak bone while holding it against visible light (7). This indicated that red light and NIR light with longer wavelengths penetrate the scalp and skull to reach the underlying tissues. Utilizing the transparency of the skin and bones to NIR light, the fNIRS technology has been utilized in a variety of fields and applications.

NIR light is transmitted onto the scalp to perform fNIRS measurements. NIR light must pass through the skin of the scalp, skull, and the cerebrospinal fluid before reaching the brain, and each of these layers has different optical properties. The light transmitted into the head will be scattered, diffused, and will be able to penetrate several centimeters through the tissue (Figure 2.1). Therefore, collecting backscattered light can be possible by placing a light detector at a certain distance from the light source. Within the NIR optical window, hemoglobin is the most dominant and physiologically-dependent absorber. As absorption within the NIR optical window is primarily attributable to HbO and HbR, changes in light attenuation at a given wavelength can be expressed as a linear combination of changes in HbO and HbR concentrations.

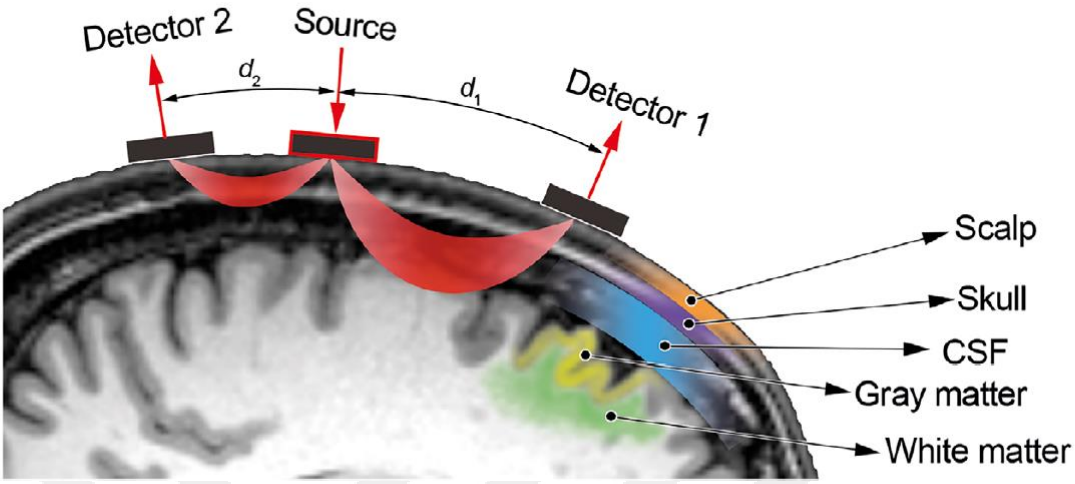

Figure 2.1. Illustration of the path (shown in red) followed by the NIR photons from the light source to the detector through the different layers of the head. The penetration depth of the light is proportional to the source–detector distance (d1: deeper channel; d2: superficial channel). A channel is composed by the pair source–detector and is located at the midpoint between the source and the detector and at a depth of around the half of the source–detector separation (37).

3. MATERIALS AND METHODS

3.1. Experimental Design

3.1.1. Participants

38 IMP (28 females, mean age 15.6±2.4 years) and 33 NIC subjects (23 females, mean age 15.1±1.9 years) with no history of neurological diseases, visual or motor dysfunction participated in the study after giving written informed consent in accordance with the latest Declaration of Helsinki. The study was approved by the Kocaeli University Ethical Committee of Clinical Research.

Due to the poor signal quality of fNIRS data, one subject from each group had been excluded. Therefore, 37 IMP and 32 NIC subjects were included in the analysis.

3.1.2. Clinical Assessment

Prof. Orhan Derman, an adolescent medicine specialist, performed the clinical assessments of all subjects. Prof. Derman determined the presence or absence of impulsivity, and each subject was labeled with binary scores (1: existence, 0: absence of impulsivity). Also, the clinical dataset (CL_{all}) which consisted of the features that conventionally had the greatest impact on the clinician’s decision-making process in clinical practice was generated by Prof. Derman. The clinical dataset includes binary scores of the following states (1: existence, 0: absence): anxiety, chronic disorders, distractibility (i.e., attention deficiency), drug use, dyslexia, eating disorder, exposure to violence, puberty disorders, self-harm or violent behavior, and smoking status.

The percent presence of the clinical features in both IMP and NIC groups are given in Table 3.1. Between the IMP and NIC groups, there were statistically significant differences in anxiety, chronic disorders, puberty disorder, and smoking status features (chi-square test, $p<0.01$).

Table 3.1. Percent presence of the clinical features in impulsive and non-impulsive groups.

Feature Name	**IMP**	**NIC**
Anxiety	54.05	0.00
Chronic disorders	10.81	37.50
Distractibility	18.92	6.25
Drug use	2.70	6.25
Dyslexia	0.00	6.25
Eating disorder	27.03	12.50
Exposure to violence	2.70	0.00
Puberty disorders	2.70	28.13
Self-harm or violent behavior	10.81	0.00
Smoking	18.92	0.00

3.1.3. fNIRS Data Acquisition

The fNIRS data were acquired using a continuous-wave multi-channel fNIRS measurement system (ARGES-CEREBRO, Hemosoft Information Technology and Training Services Inc., Ankara, Turkey) (38–42). This system is equipped with a head probe that contains 4 dual-wavelength (730 and 850nm) light sources and 10 photodetectors designed to cover the forehead. With a fixed source-detector distance of 2.5cm, this configuration generates a total of 16 channels per wavelength. To detect the hemodynamic activity in the PFC region, the head probe was placed on the forehead such that the bottom row of the detectors was just above the eyebrows. The probe configuration and channel distribution are shown in Figure 3.1. It has been shown that each light source is able to penetrate the scalp while transmitting near-infrared light at two wavelengths (730 and 850nm) and can be used to probe a portion of the dorsolateral, orbitofrontal, and medial PFC regions (43). Detectors record relative changes in HbO and HbR with a sampling frequency of 2.5 Hz at two wavelengths. The concentration changes in HbO and HbR signals are calculated from the modified Beer-Lambert law using two wavelengths.

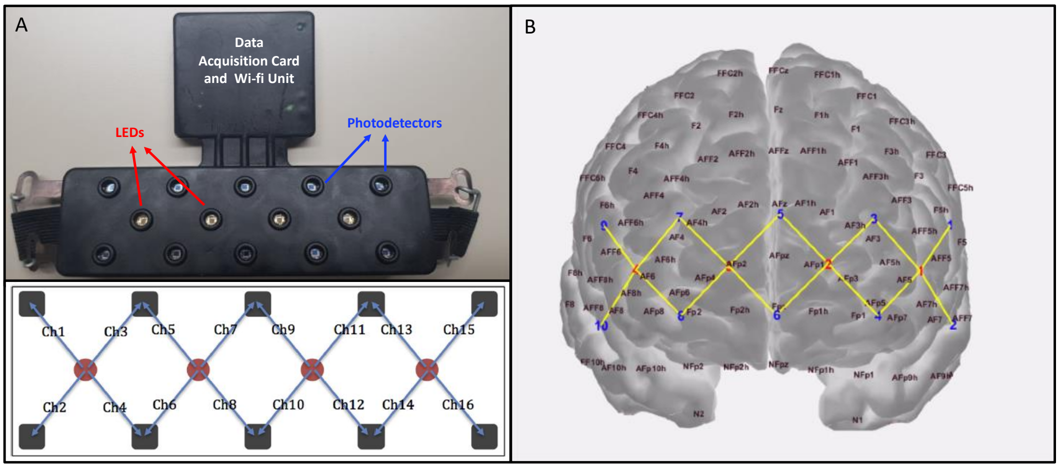

Figure 3.1. A) Configuration of the forehead probe B) approximate location of the LEDs and photodetectors with respect to the international 10-20 system for electrode placement. LEDs are demonstrated with red dots and detectors are represented with blue dots. Yellow lines are drawn between the LED-photodetector pairs which form channels.

3.1.4. Experimental Paradigm

Subjects were seated in a comfortable chair in front of a computer screen positioned approximately 1m apart from the subject's eyes in a silent, dimly lighted room. They were asked to relax and refrain from any movement as much as possible during the experiment. Subjects were asked to perform a Turkish version of the SCWT (44) in a block design. The experimental paradigm consisted of three different types of stimuli, namely neutral stimulus (N), congruent stimulus (C), and incongruent stimulus (IC). An experimental run consisted of 3 stimulus blocks (N, C, and IC) and each stimulus block consisted of 20 trials with an interstimulus interval of 3 seconds. Each stimulus block was separated with a 15 second rest period. A white crosshair with a black background appeared on the screen between the interstimulus intervals. Each subject's order of task blocks was randomized. Within each block, the types of trials were identical, but the presentation of correct and false trials was randomized.

Two rows of letters are displayed on the screen, for each type of trial. The top one was written in ink color whereas the bottom one was in white. Subjects were asked to judge whether the color of the top row letters corresponded to the meaning of the word displayed at the bottom row. Subjects gave their responses by pressing either the left button of a mouse with their right index finger or the right button of a mouse with their middle finger for matching and non-matching conditions respectively (Figure 3.2). Subjects were instructed to perform the task as quickly and correctly as possible.

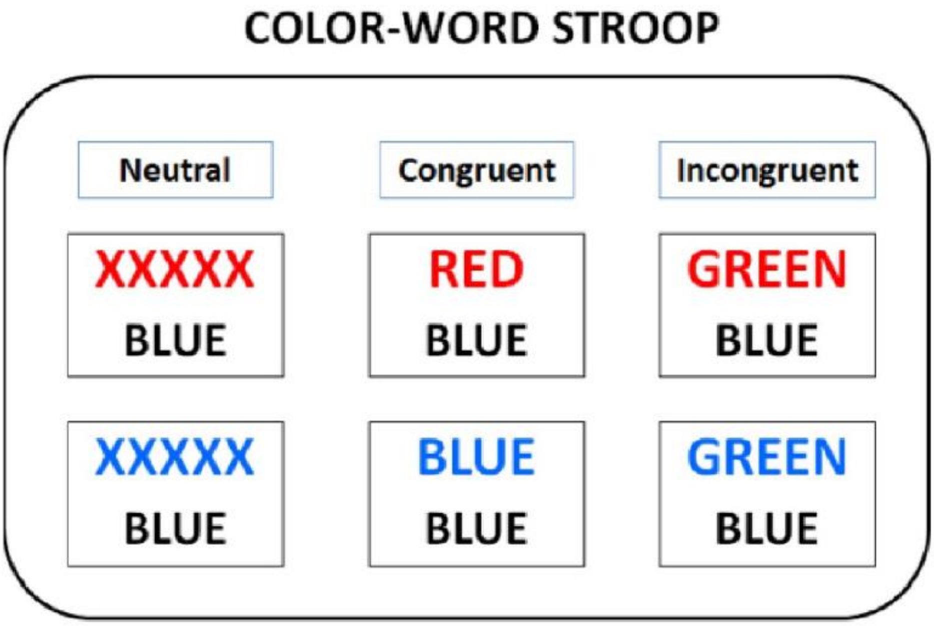

Figure 3.2. Stimulus conditions presented during the color-word matching Stroop task. The words in the upper row present non-matching (i.e., the word below wrongly defines the color of the word above in each box) cases for neutral (N), congruent (C), and incongruent (IC) conditions. Similarly, the words presented in the second row present the match cases for the three conditions where the word presented below correctly defines the color of the word above in each box.

In the N trials, the letters “XXXXX” appeared in blue, green, red, or yellow in the top row and the bottom row comprised of Turkish names of color words of ‘BLUE’, ‘GREEN’, ‘RED’ or ‘YELLOW’ appeared in white. In the C trials, Turkish names of color words of ‘BLUE’, ‘GREEN’, ‘RED’ or ‘YELLOW’ appeared in the top row printed in congruent color. In the IC trials, the color word that appeared in the top row was printed in a different color than the word’s meaning to produce interference between coloring the word and naming it (45).

3.2. Data Analysis

3.2.1. fNIRS Data Preprocessing

Data preprocessing was performed in MATLAB R2017a (Mathworks, Natick, MA, USA) with custom-written scripts. To extract neuronal information from fNIRS data, any source of variability in both HbO and HbR signals that is not related to task-evoked hemodynamic activity needs to be eliminated or minimized. Only the change in HbO concentration is used for further analysis in the proposed study because a higher signal-to-noise ratio has been reported for HbO signals (46–48), and HbO signals have also been reported to be a more reliable indicator of cortical activation (46,49,50).

A partial correlation (PC) analysis was performed to eliminate systemic physiological noise. By applying the PC analysis to the HbO time series data, the correlation between each channel pair's time series was computed after regressing out the interference of a third variable that has a common and undesired interference on both channels. This common and undesired variable is regarded as the global systemic noise embedded in each channel's HbO data. The partial correlation regressor was calculated by averaging the 0.009Hz high pass filtered HbO signals of all channels.

To obtain data for each stimulus condition, the full-length HbO time series was truncated from the onset to the end of each stimulus block. Truncated time traces belonging to each block of the same condition were concatenated to form a single time series for that condition. Thus, a total of three separate HbO time series belonging to each stimulus condition were obtained for each channel of each subject. PC coefficients between any two channel pairs were computed for each stimulus condition separately.

3.2.2. Computation of Global Efficiency, Neural Efficiency and Cognitive Quotient Features

FC refers to the premise that functionally related brain regions generate correlated and coherent signals both during rest and when neuronally engaged in a cognitive task (51,52). Consequently, FC-based metrics are regarded as an indicator of the degree of connectivity or the efficiency of information transfer between different brain regions. Scarpino (2017), asserts that the performance metrics of the Stroop test would assess several executive functions including inhibition, attention, processing speed, and cognitive flexibility (53). During the Stroop task, multiple PFC regions attend to the processing of information in coordination. Consequently, FC-based metrics are thought to represent the extent of PFC engagement during various types of trials.

Global Efficiency (GE), a graph theory-based metric, was computed to quantify the effectiveness of functional connectivity in the PFC (45,54). First, the partial correlation between each channel pair was computed using the time series data for each stimulus that had been preprocessed. Then, 16 by 16 correlation matrices were formed from the correlation coefficients between truncated time series of each possible pair for each stimulus condition and each subject. The channels and the partial correlation coefficients were assigned as a set of vertices and weights on the set of edges in the graph-based network analysis, respectively. The Latora and Marchiori efficiency measure (55) was used to compute the GE values as follows:

$$GE = \frac{1}{N(N-1)} \sum_{i \neq j \in G} \frac{1}{d_{ij}}$$

where d_{ij} is “defined as the smallest sum of the physical distances throughout all the possible paths in the graph from i to j.” (56).

Another neurophysiological metric, Neural Efficiency (NE), is considered to provide discriminatory information between the two subject groups by combining behavioral and hemodynamic measures. According to the neural efficiency hypothesis of intelligence (NEH), more intelligent individuals' brains consume less energy when performing simple cognitive tasks but more energy when engaged in difficult mental operations (57). This neural capacity of more intelligent individuals to respond discriminatively to situational challenges by less allocation of neural resources can be most prominently seen in the PFC, the seat of executive functioning (58). Additionally, it has been suggested that more intelligent individuals are able to perform the same cognitive performance with less energy when compared to less intelligent individuals (46,47,54).

Based on NEH, a cognitive quotient (CQ) metric was proposed to evaluate the overall cognitive performance during each stimulus condition for each subject. The CQ was calculated by dividing the accuracy (percentage of correct answers) to the average reaction time of that specific stimulus condition. NE of each stimulus condition was then calculated for each subject by multiplying the CQ by the GE for that stimulus condition. Stroop interference of the NE and CQ was calculated as the difference between the IC and N conditions, and IC and C conditions of each metric.

3.2.3. Feature Extraction

The behavioral dataset (BEH_{all}) consists of accuracy (ACC) response time (RT), and CQ metrics for each stimulus condition. The ACC and RT metrics for each stimulus condition were computed as the percentage of correct answers and average response time for the trials belonging to the specific stimulus condition, respectively. The hemodynamic dataset ($HEMO_{all}$) was composed of GE and NE metrics for each stimulus condition. Additionally, the Stroop interference was computed for NE and CQ metrics (NE_{IC-N}, NE_{IC-C}, CQ_{IC-N}, and CQ_{IC-C}). Table 3.2. presents descriptive statistics for the behavioral and hemodynamic dataset arranged by subject group.

Table 3.2. Summary of BEH_{all} and $HEMO_{all}$ features used to feed the ML algorithms.

	Feature Name	**IMP**	**NIC**
Behavioral Features	Accuracy-Neutral (%)	92.3 ± 8.38	91.72 ± 8.85
	Accuracy-Congruent (%)	96.35 ± 3.66	95.94 ± 5.45
	Accuracy-Incongruent (%)	90.41 ±11.69	93.59 ± 6.38
	Reaction Time-Neutral (s)	1.29 ± 0.20	1.23 ± 0.23
	Reaction Time-Congruent (s)	1.14 ± 0.19	1.09 ± 0.17
	Reaction Time-Incongruent (s)	1.41 ± 0.26	1.43 ± 0.28
	Cognitive Quotient-Neutral	73.60 ± 13.96	78.30 ± 20.18
	Cognitive Quotient-Congruent	86.44 ± 14.53	90.51 ± 16.27
	Cognitive Quotient-Incongruent	67.05 ± 16.71	68.14 ± 15.16
Hemodynamic Features	Global Efficiency-Neutral	0.30 ± 0.07	0.32 ± 0.07
	Global Efficiency-Congruent	0.30 ± 0.07	0.32 ± 0.07
	Global Efficiency-Incongruent	0.28 ± 0.07	0.30 ± 0.07
	Global Efficiency Interference (IC-N)	−0.03 ± 0.06	0.02 ± 0.09
	Global Efficiency Interference (IC-C)	−0.02 ± 0.09	−0.01 ± 0.08
	Neural Efficiency-Neutral	22.19 ± 6.29	25.53 ± 9.38
	Neural Efficiency-Congruent	25.94 ± 7.59	29.38 ± 10.06
	Neural Efficiency-Incongruent	18.35 ± 5.86	21.09 ± 8.04
	Neural Efficiency Interference (IC-N)	−3.85 ± 6.67	−4.44 ± 6.83
	Neural Efficiency Interference (IC-C)	−7.59 ± 8.69	−8.29 ± 9.48

3.2.4. Classification Methods

SVM and ANN algorithms were used to test the feasibility of correctly classifying the IMP and NIC subjects using features from multiple domains.

These algorithms were chosen because of their low computational cost and demonstrated ability to perform well with small sample sizes (n<200) in both previous fNIRS-based BCI studies (49,50,56,57,59,60) and related applications in other fields (61,62). The WEKA data mining software (version 3.8.4) (63) was used in the classification of IMP and NIC subjects with the clinical, behavioral, and hemodynamic datasets and their combinations.

3.2.4.1. Support Vector Machines

SVM is a widely used supervised machine learning classification algorithm introduced in 1992 by Boser et al. SVMs are based on the generation of a hyperplane that can best separate data into classes (64). The SVM predicts the hyperplanes iteratively to determine the optimal hyperplane that minimizes the error. Optimization of this hyperplane is established by minimizing the error function:

$$J(\omega, \xi) = \frac{1}{2}\left||\omega|\right|^2 + C\sum_{i=1}^{N}\xi_i$$

while satisfying the constraints:

$$y_i\left(\omega^T \emptyset(x_i)\right) + b \geq 1 - \xi_i, \qquad \xi_i \geq 0$$

In these equations, ω is a coefficient vector defining the weights assigned to each feature stored in x_i, b is a scalar and ξ_i is the slack variable which holds the distance measures between the margins. Index i goes through all N training sets. y_i represents class labels (−1 or 1) and x_i is a vector that represents the independent variables or in other words, the features. C is a positive regularization parameter which optimizes the presence of outliers and reduces errors in the training and test set.

This hyperplane is employed on new datasets to properly classify them. If the data points belonging to each class are linearly separable, all data can be classified with a single hyperplane. However, if data cannot be separated linearly, they often cannot be classified with a single plane. The kernel trick provides a solution to this issue. The kernel trick is used to transform a low-dimensional input space into a higher-dimensional space. In other words, by adding more dimensions to the problem, the kernel transforms non-separable problems into separable ones. This makes SVM classifiers flexible, very powerful, and accurate. Some of the common kernels used with SVM can be listed as linear kernel, polynomial kernel, Radial Basis Function (RBF) kernel, and Pearson VII kernel (PUK).

Platt (1998) proposed the sequential minimal optimization (SMO) algorithm for training the SVM classifier and applied it to minimize the complexity of the SVM optimization problem (65). The WEKA SMO classifier was run 10 times with 10-fold cross-validation using the Radial Basis Function kernel with default parameters (C=1, γ=1).

3.2.4.2. Artificial Neural Networks

ANN is a popular machine learning technique inspired by the operating basics of the biological neural network of the human brain (66). ANN is especially suitable for complex non-linear information processing systems thanks to its self-adaptive and self-learning functions. A general neural network comprises of one input layer, one or more hidden layers, and one output layer. A commonly used type of ANN, feed-forward neural networks (67), assign weights to each artificial neuron, which receives inputs from neurons in the previous layer and transmits its processed output to the next layer. Multilayer Perceptron (MLP) (68) is a significant type of feed-forward neural network. The most prevalent MLP training technique is the back-propagation algorithm (BPA), which iteratively adjusts the weights between neurons to minimize prediction error. This model is exceptional in pattern recognition. Although BPA can easily adapt to newly added data points, its slow convergence rate and risk of becoming trapped in a local optimum pose a problem (69). In addition, deciding the structure of the algorithm, the number of layers and number of hidden neurons in each layer, and the connectivity between them all have a significant impact on the performance of the neural network. Therefore, even a slight variation in any of these parameters can have a significant impact on the result. Different ANN architectures will yield different results for different problems. Application problems will always necessarily require a structure that provides near-optimal results. However, achieving an optimal ANN architecture through trial and error is a challenging task.

The Multilayer Perceptron classifier was run 10 times with 10-fold cross-validation in WEKA using the default parameters (single hidden layer, learning rate of 0.3, and training time of 500 epochs) to reduce the possibility of overfitting. By default, WEKA computes the number of neurons in the hidden layer as the mean of the number of neurons in the input and output layers. The activation function used in the model is the sigmoid function shown as:

$$f(x) = \frac{1}{1 + e^{-x}}$$

3.2.5. Feature Selection

In a classification study, we need numerous features that define the sample group. However, this does not always mean that 'the more the merrier'. Feeding the classification algorithm with uninformative and redundant features can distort the classification performance. Feature selection methods are used to prevent the classification algorithms from redundant and uninformative features. Feature selection methods can be categorized into 4 basic groups of methods which are i) filter, ii) wrapper, iii) embedded, and iv) hybrid methods. In this study, the wrapper feature selection method was used with the evaluation measure of accuracy to find the best set of features. Feature selection was applied to clinical, behavioral, and hemodynamic datasets individually and using each classification algorithm separately. The wrapper-based feature selection was run for 5 times with 10-fold cross-validation with the same parameters used in classification algorithms.

The resultant weights for each feature were averaged across all 5 runs. The three features with the highest weights from each domain were selected to create new datasets that composed of the selected features. The classification accuracy of each algorithm when fed with CL_{all}, BEH_{all}, and $HEMO_{all}$ and their combinations, and CL_{sf}, BEH_{sf}, and $HEMO_{sf}$ and their combinations were compared.

4. RESULTS

In this section, the accuracy performances of SVM and ANN classifiers using all the features from different domains and their combinations are presented first, followed by their accuracy performances when trained with i) the selected features from the three domains separately and ii) different combinations of selected features from the three domains.

4.1. Classification Performance with All Features

In this case, both classifiers were fed with all the features of the clinical, behavioral, and hemodynamic datasets (CL_{all}, BEH_{all}, and $HEMO_{all}$, respectively) and their combinations. Since features of the CL dataset have the greatest impact on the clinician's decision-making process in conventional practice, the performance of the CL_{all} dataset was considered as a reference. The accuracy of the SVM and ANN classifiers when fed with CL_{all}, BEH_{all}, and $HEMO_{all}$ and their combinations are demonstrated in Table 4.1.

Table 4.1. Accuracy performances (mean ± standard deviation) of SVM and ANN classifiers when trained with all features in the different feature set combinations. p-values denote statistical significance of the difference between performances of SVM and ANN classifiers when fed with the feature set combination named at the top of each column. $p<0.05$ are denoted with an asterisk (∗).

	CL_{all}	BEH_{all}	HEM_{all}	CL_{all}+BEH_{all}	CL_{all}+$HEMO_{all}$	BEH_{all}+$HEMO_{all}$	ALL
SVM	88.12±1.14	54.35±3.15	55.8±2.67	88.26±1.06	87.4±2.06	56.81±3.26	88.55±1.44
ANN	89±0.74	60±9.82	51.45±6.27	88.26±2.5	84.39±1.49	53.91±5.01	86.82±2.21
p-value	0.052	0.006*	0.721	0.999	0.01*	0.57	0.44

Using the CL_{all} dataset with the SVM classifier resulted in a classification accuracy of 88.12±1.14%. Pooling all features of all datasets (CL_{all}+BEH_{all}+$HEMO_{all}$ or ALL in short) increased the accuracy of the SVM slightly and resulted in an 88.55±1.44% classification accuracy. However, this increase was not statistically significant. Feeding the ANN with the ALL dataset resulted in a decrease in accuracy (86.82±2.21%) compared to the performance of the ANN when fed with the CL_{all} (89±0.74%). Similar to the change in the SVM classifier, this decrease was not statistically significant. The addition of features that are possibly irrelevant, redundant, and not useful for differentiating the two groups may confuse the learning algorithms and cause non-significant improvements in classification performance. In the majority of instances (Table 4.1.), there were no statistically significant differences between the accuracy performances of the SVM and ANN. Both classifiers were able to classify the data with an accuracy above 84% when fed with CL_{all}, CL_{all}+BEH_{all}, CL_{all}+$HEMO_{all}$, and ALL datasets. Even though the mathematical architectures of the SVM and ANN are very different, these similar accuracy results show that the listed features are inherently distinctive. It also emphasizes the feasibility of both algorithms in classifying IMP and NIC accurately when fed with listed features.

4.2. Classification Performance with Selected Features

In this case, CL_{sf}, BEH_{sf}, and $HEMO_{sf}$ datasets and their possible combinations were utilized for training purposes. For each classifier, wrapper-based feature selection is applied to the feature set of each domain individually to identify the most informative, independent, and relevant feature subsets that maximize the accuracy of the classifier while eliminating the redundant and uninformative features that distort the classification accuracy. Therefore, an improvement in the accuracy of both classifiers was expected when fed with datasets that consist of selected features. The classification accuracy of the SVM and ANN, when fed with the datasets that consist of selected features (CL_{sf}, BEH_{sf}, and $HEMO_{sf}$) and their combinations are given in Table 4.2.

Table 4.2. Accuracy performances (mean ± standard deviation) of SVM and ANN classifiers when trained with selected features in the different feature set combinations. p-values denote statistical significance of the difference between performances of SVM and ANN classifiers when fed with the feature set combination named at the top of each column. $p<0.05$ are denoted with an asterisk (∗).

	CL_{sf}	BEH_{sf}	HEM_{sf}	$CL_{sf}+BEH_{sf}$	$CL_{sf}+HEMO_{sf}$	$BEH_{sf}+HEMO_{sf}$	ALL_{sf}
SVM	89.34±0.89	55.36±2.45	61.6±2.45	89.57±1.5	91.61±1.24	61.05±2.02	92.16±0.7
ANN	88.28±3.42	56.52±2.65	56.52±2.65	88.7±2.44	89.13±1.56	60±2.75	90.35±1.71
p-value	0.353	0.0001*	0.0001*	0.350	0.001*	0.346	0.006*

The features that were selected by wrapper-based feature selection using the SVM and ANN have listed in Table 4.3. The variety of features that are selected for each algorithm highlights the importance of including multiple stimulus types for extracting hemodynamic and behavioral responses from the subject population since each algorithm may emphasize a different distinctive property of each feature across the subject population.

Table 4.3. Summary of selected features using the SVM and ANN.

	SVM	ANN
CL_{sf}	Smoking status	
	Anxiety	
	Eating disorder	
BEH_{sf}	Reaction Time-Neutral	Cognitive Quotient-Neutral
	Cognitive Quotient-Neutral	Reaction Time-Incongruent
	Accuracy-Congruent	Accuracy-Incongruent
$HEMO_{sf}$	Neural Efficiency-Neutral	Neural Efficiency-Neutral
	Cognitive Quotient-Congruent	Neural Efficiency-Congruent
	Global Efficiency-Incongruent	Global Efficiency Interference (IC-C)

The effect of wrapper-based feature selection was tested with paired t-tests that compared the classification accuracy of each algorithm when fed with CL_{all}, BEH_{all}, and $HEMO_{all}$ and their combinations, and CL_{sf}, BEH_{sf}, and $HEMO_{sf}$ and their combinations. Feature selection improved the SVM's classification accuracy for all of the feature sets. Besides, for the ANN, except for the clinical-only dataset, an increase in classification accuracy also occurred by the use of feature selection. Thus, for most of the predictive models (classifier-feature set combination), wrapper-based feature selection revealed an increase in classification accuracy.

When the CL_{all} dataset is fed to the SVM and ANN classifiers, as is conventionally used in the clinician's decision-making process, the accuracy performances were 88.12±1.14% and 89±0.74%, respectively. On the other hand, the accuracy performances of SVM and ANN were revealed as 92.16±0.7% and 90.35±1.17%, respectively, when fed with the combination of the selected features of each domain (ALL_{sf}). Figure 4.1. shows a comparison of the classification accuracy of the SVM and ANN algorithms when fed with the CL_{all} and ALL_{sf}. Feeding the classifier algorithms with the ALL_{sf} resulted in an increase in the accuracy performance of both SVM ($p<0.01$) and ANN ($p=0.2$) compared to feeding each algorithm with the CL_{all} dataset.

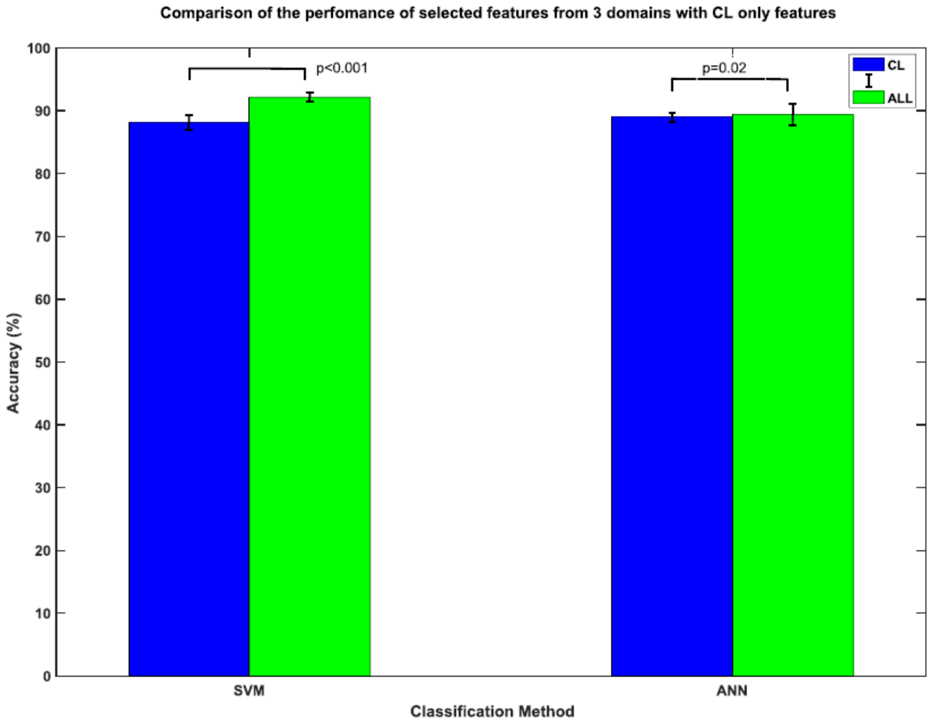

Figure 4.1. Comparison of the performances of SVM and ANN classification algorithms when trained with (a) CL_{all} dataset and (b) ALL_{sf}.

Although using ALL_{sf} increased the accuracy of both classifiers, the improvement in accuracy is more distinct for the SVM. Furthermore, using the ALL_{sf} revealed a statistically significant difference between the classification accuracies of the SVM and ANN (p=0.006). Both classifiers performed comparably well, but the SVM showed statistically significantly higher accuracy with the ALL_{sf} when compared to the ANN.

5. DISCUSSION

In clinical practice, impulsivity is diagnosed using qualitative measures, including structured interviews, self-reports (i.e., the Barratt impulsiveness scale (3)), questionnaires, and neuropsychological tests. Inaccurate diagnosis may be caused by the fact that subjects may have difficulty in deciding which specific information to share and/or they may disguise the actual information. In addition, the clinician's interpretation of the data obtained from conventional methods introduces subjectivity and may challenge the accuracy of clinical diagnosis. Considering these factors, it is evident that there is a demand for an objective and reliable system for an accurate diagnosis. In line with this demand, this study aimed to assess the feasibility of an fNIRS-based BCI system by using ML approaches for accurate identification of impulsivity in adolescents. For this purpose, classification models were constructed with two commonly used and computationally efficient classifiers, SVM and ANN, which have been shown to perform well with small sample sizes (n<200) in previous studies (20,70–77).

Aspects of impulsivity are associated with inadequate motor planning, lack of attention, and/or lack of forethought (1). Considering the multifaceted nature of impulsivity in addition to its multifactorial etiology, it is proposed that training the SVM and ANN classifiers with features from clinical, behavioral, and hemodynamic domains could better elucidate the neurobiology underlying the symptoms when attempting to identify impulsivity at the individual level. It is anticipated that the combination of features from different domains would improve the classification accuracy when compared to the use of clinical questionnaire-derived features alone. SVM and ANN were evaluated to classify IMP and NIC using different feature sets and their combinations. Each prediction model's accuracy performance was evaluated with and without a feature selection procedure to eliminate redundant or uninformative features that may distort classification accuracy.

A novel method for computing FC-based features from the hemodynamic activity of PFC was developed, and the NE metric was derived by combining behavioral metrics and FC measures. The accuracy of two commonly used classifiers was evaluated for identifying IMP and NIC subjects using feature sets from the clinical, behavioral, and hemodynamic domains.

The proposed system can acquire behavioral performance metrics and cortical hemodynamic activity data during a neuropsychological test with the outcome of conventionally utilized clinical questionaries may facilitate the clinical practice of accurate diagnosis and/or assist the clinician's diagnosis by providing a decision outcome that is obtained by training machine learning algorithms based on the decision of an experienced clinician. The findings contribute to the idea of development of an objective assessment of impulsivity and suggest the potential of a computer-aided diagnosis perspective for a reliable rating of the severity by combining metrics from the clinical, behavioral, and hemodynamic domains. No studies to date have attempted to classify impulsivity using novel FC-based features and neuropsychological data simultaneously. In addition, no study in the current literature proposes the use of multidomain biomarkers of impulsivity for classification purposes by combining fNIRS-based neurophysiological features with behavioral and clinical metrics. This study contributes to the development of an objective measure of impulsivity and suggests the investigation of biomarkers based on fNIRS. Even when trained with small sample sizes, our results demonstrated the promise of MVPA methods for accurately identifying impulsivity at the individual level.

The remainder of this section is divided into 4 subsections. First, the performance of SVM and ANN classifiers were evaluated when they were trained with CL, BEH, and HEMO features and the performance of feeding each algorithm with different combinations of feature sets are compared. Interpretation of this analysis is concluded by emphasizing the importance of including a feature selection approach. Potential reasons for the poor performance of the mentioned algorithms in classifying IMP from HC when fed with BEH and HEMO features are discussed, and strategies are proposed to improve their performance for future studies.

5.1. Comparison of the Accuracy Performances of the SVM and ANN

Both SVM and ANN achieved classification accuracy above 90% when fed with the classifier-specific ALL_{sf} datasets. Although both algorithms had performed well in classification, the SVM showed statistically significantly higher accuracy than ANN ($p=0.005$). High classification accuracies obtained from both the SVM and the ANN when fed with the combination of selected features from each domain emphasize the applicability of ML-based classification approaches for objective identification of impulsivity. The similar and high accuracy performances of both the SVM and ANN in classification of IMP and NIC demonstrate that selected features from each domain are inherently distinctive, despite the fact that the mathematical architectures of these algorithms are very different. ML-based classification approaches for automated discrimination of neurological and psychiatric disorders have gain in popularity over the last decade. Most of these studies investigated the diagnostic value of developing models that use multivariate structural and functional neuroimaging measures to discriminate patients from controls.

In the past decade, there has been an increasing interest in the exploration of ML-based classification approaches for automated discrimination of neurological and psychiatric disorders. Most of these studies focused on examining the diagnostic value of building models that utilize multivariate structural and functional neuroimaging measures for the ultimate goal of discriminating patients from their healthy counterparts. Studies that reported the classification performance of SVM in discriminating patients with psychiatric disorders from healthy subjects were summarized by Orru et al. (26). Classification accuracies reported in Orru et al. (2012), were in the range of 67% and 100% and were affected by many factors including sample size, type of resampling procedure, type of kernel being used, type of disorder, and type of parameters (26). Compared to the performances reported for the classification of various psychiatric disorder populations, the accuracy metrics obtained with the classification approach in this study remain within the high-performance range.

No previous research has evaluated the feasibility of using an automated classification algorithm to identify impulsivity. However, it is still possible to compare the accuracy performances of this study and previous studies that aimed to distinguish ADHD patients from controls using multi-domain features. Crippa et al. (23) used the PFC activation metrics obtained from fNIRS and reached a maximum accuracy of 81% with the SVM whereas Zhu et al. (78) reached an accuracy of 85% by feeding the SVM with PFC activation metrics obtained from fMRI. Due to the accuracy performance of the proposed model, it can be said that it outperformed previously reported accuracy performances in ADHD studies.

5.2. Limited Contribution of Behavioral and Hemodynamic Features to the Accuracy Performance

The accuracy performances of both SVM and ANN, when fed with the CL_{all} dataset, were considered as a reference since the features of the CL_{all} dataset have the greatest impact on the clinician's decision-making process in conventional practice. The SVM and ANN achieved a classification accuracy of 88% and 89%, respectively, when fed the CL_{all} dataset. Fusing CL_{all}, BEH_{all}, and $HEMO_{all}$ improved the classification accuracy by approximately 4% and 1%, respectively. The improvement in classification accuracy of both SVM and ANN was statistically significant. However, when both classification algorithms were fed with the BEH and HEMO datasets by themselves, they could not reach a classification accuracy above 70%, which is the minimum reportable accuracy in binary classification. The relatively modest performance of BEH and HEMO datasets raises the question of whether the Stroop test was adequate to obtain predictive behavioral metrics of impulsivity and whether the fNIRS-based NE and GE were the 'right' features to achieve good classification accuracy.

Subjects were required to suppress processing of the meaning of the word presented on the top row and focus on reading the ink color of the word during the color-word Stroop test. In IC stimuli, naming the ink color was expected to take a longer time than naming the ink color in N and C stimuli. Therefore, the performance metrics of the test would be closely related to various executive functions, including behavioral conflict resolution, response inhibition, cognitive flexibility, cognitive interference, and selective attention skills. However, a portion of the multifactorial etiology of impulsivity can be spanned by the Stroop test measures, such as aspects related to inadequate motor planning, lack of attention, and/or lack of forethought. This limited span can be expanded by including several tests to the neuropsychological test battery that aim at the employment of a variety of cognitive abilities, i.e., the Go/No-Go test, the Wisconsin Card Sorting test, the London Tower test, and the Stop Signal task. Using an experiment set that combines such an extensive neuropsychological test battery and an fNIRS-based BCI system, more discriminative features can be extracted. Additionally, a larger cohort of participants will enable the exploration of the classification of the severity of impulsivity and/or improve the classification performance.

Functional activation of the frontal brain regions and alterations in FC in children with ADHD compared to control subjects have been demonstrated in recent literature (18–25). During the Stroop tasks, processing in multiple PFC regions needed to be in coordination. Thus, the GE metrics were considered to provide a good representation of the activation of the overall PFC regions (79). However, using functional activity localization based features can also improve the classification performance. The HbR and total hemoglobin (HbT) signals can also be used to extract new features. These features can be used to feed the classification algorithms alone or can be fused with the HbO-derived features.

5.3. Importance of the Findings

This study aimed to propose an fNIRS-based BCI system that would assist clinicians in the identification and diagnosis of impulsivity in adolescents. Feeding the classification algorithms with the combination of novel fNIRS-based features and the features obtained from the clinical questionary and the Stroop test may improve the correct diagnosis of impulsivity.

Impulsivity has a multifactorial nature, and it has aspects related to inadequate motor planning, lack of attention, and/or lack of forethought. Thus, fusing informative features obtained from CL, BEH, and HEMO domains would be more descriptive while using features from a single domain would span only a portion of the multifaced nature of the impulsivity. Indeed, feeding SVM and ANN with the combination of CL_{all}, BEH_{all}, and $HEMO_{all}$ improved the classification accuracy by approximately 4% and 1%, respectively. These improvements are statistically significant. Hence, classification performance of IMP and NIC using the informative multidomain features was considerably higher than using only the CL_{all} dataset. Inaccurate diagnosis may be caused by the fact that subjects may have difficulty in deciding which specific information to share and/or they may disguise the actual information. In addition, the clinician's interpretation of the data obtained from conventional methods introduces subjectivity and may challenge clinical diagnosis. Considering these factors, it is evident that there is a demand for an objective and reliable decision support system for accurate diagnosis. In line with this demand, this study aimed to assess the feasibility of an fNIRS-based BCI system using machine learning approaches for the accurate identification of impulsivity in adolescents. One handicap of diagnosing impulsivity using only clinical data obtained from self-reports or questionnaires is the potential risk of getting manipulated information from subjects. Another handicap of using only self-reports or questionnaires is that the diagnostic procedure may be influenced by the practical knowledge and experience of the clinician, so the procedure may differ from clinician to clinician, besides the clinician's interpretation of the data obtained from conventional methods introduces subjectivity and may challenge clinical diagnosis. Thus, feeding the classification algorithms with objective and informative features extracted from a neuropsychological test and neuroimaging system would improve the performance of decision support system designs similar to the system proposed in this study. It is believed that any improvement in the performance of such a decision support system by the use of multidomain features is valuable since impulsivity has a multifactorial nature in many aspects.

The preliminary results of this study contribute to the development of an objective assessment of impulsivity and suggest the potential of a computer-aided diagnosis perspective for a reliable rating of the severity by combining metrics from the clinical, behavioral, and hemodynamic domains. They also indicated that MVPA methods can be used effectively to identify impulsivity in adolescents. Such systems, similar to the proposed system in this study, can be easily implemented in clinics and may facilitate the clinical practice of accurate diagnosis and/or assist the clinician in diagnosing. Likewise, implementation of such a system in high school settings may help the consultancy teachers in directing the students at high risk of impulsivity to clinics at the right time.

Results indicate the feasibility of ML-based classification approaches for the objective identification of impulsivity by using multidomain features. The findings contribute to the idea of the development of an objective assessment of impulsivity and suggest the potential of a computer-aided diagnosis perspective for a reliable rating of the severity by combining metrics from the clinical, behavioral, and hemodynamic domains. Considering its high prevalence, clinical heterogeneity, and societal costs, the diagnosis of impulsivity may soon benefit from more predictive analytics, as these neuroimaging-assisted techniques will continue to evolve by combining optimal neuropsychological test batteries, signal processing strategies, feature extraction, and feature selection procedures.

5.4. Limitations of the Study and Recommendation for Future Work

Although the results are promising, this study has several limitations. The sample size of this study exceeds many of the classification studies in neuropsychiatry literature. However, it was still small compared to the ML studies conducted on big data. Future work will concentrate on validating the proposed system design on larger sample groups. This study focused on the identification of impulsivity in only adolescents, so the findings cannot be generalized to other age groups. A subject group who has comorbidity of disorders should be also included in the study for testing the disorder specificity of the proposed system. Thus, expanding the sample size by including participants from other age groups and participants who have the comorbidity of disorders is very crucial to generalize the proposed system. While expanding the sample size, including several neuropsychological tests in the test battery that simultaneously acquire fNIRS data and extracting test-specific metrics to be used for feeding the classification algorithms would improve the performance of the system.

As the field rapidly evolves, fNIRS analysis methods are becoming more refined and more versatile. The proper exclusion of trial blocks with improper baseline state is an important concern that is frequently neglected in preprocessing procedures. Using vector phase analysis, a great method for defining trial blocks with improper baselines was proposed by Lim et al. (80). Further studies, which take this approach into account, will need to be performed. In addition, to interpret which specific regions of the brain contribute to the predictive value of the identification of impulsivity, novel features will be included in the proposed system. The dynamic nature of the brain, especially during tasks, is an important issue to keep in mind when extracting biologically informative features to represent the difference between IMP and NIC subjects. The assumption of stationarity may explain in part the complexity of the information transfer processes between distinct regions of the brain during tasks, whereas conventional FC approaches assume that different regions of the brain are connected in a static manner over temporal courses (52). FC analysis approaches evolved from static to dynamic temporal networks. Dynamic FC analysis provides valuable information on shifting connectivity states that might not have been adequately addressed by static FC analysis (81). Hence, future studies should examine the performance of classification algorithms when they are fed with dynamic FC-based features.

In this study, the feature selection procedure was performed using the wrapper method. The efficacy of the filter-based methods was also tested in the WEKA, but the classification accuracy of the algorithms, when fed with the features selected by the filter method, was significantly lower than the reported ones. Although filter-based feature selection approaches are reported to perform faster than wrapper-based methods, wrapper-based methods select the features iteratively by evaluating the predetermined performance metric with the classification algorithm. Considering all of these, the wrapper method was used since the time accuracy trade-off did not pose a significant problem in this study. Nevertheless, further work on feature selection by testing the efficacy of different approaches, including the LASSO (82), canonical correlation analysis approaches (83), and joint independent component analysis (84) would help us to enhance the proposed system.

Since the HbO signal has been reported to be more sensitive to regional changes in cerebral blood flow compared to HbR and HbT signals in previous fNIRS studies (85–87), HbO signals were used in this study. Particularly, in the fNIRS literature, HbO signals are used to present retest reliability during task paradigms (47,49). Also, HbO signals have been reported to be a more reliable indicator of cortical activation and task-related neural activity with a higher signal-to-noise ratio (46,49,50). Indeed, when the classifiers were fed with a feature set that included HbO-driven GE and NE metrics, a statistically significant increase in accuracy was observed. For future work, the same analysis should be repeated, and the efficacy and reliability of features extracted from HbR signals should also be examined with the same classification algorithms.

To sum up, further work needs to be performed in order to optimize the performance of future BCI-based decision support system study designs by testing different approaches in each step of this study. Although the proposed system has limited capacity to be considered as a substitute for clinical diagnosis decisions, promising findings show the potential of this system for improving correct diagnosis.

6. CONCLUSIONS

The ultimate goal of this study was to test the feasibility of an fNIRS-based BCI system for the accurate classification of impulsive and non-impulsive adolescents on the basis of multidomain features. Using such a system that can acquire behavioral performance metrics and cortical hemodynamic activity data during a neuropsychological test with the outcome of conventionally utilized clinical questionaries may facilitate the clinical practice of accurate diagnosis and/or assist the clinician in diagnosing by providing a decision outcome which is obtained by training machine learning algorithms based on an experienced clinician’s decision. The comorbidity of impulsivity reflects a multifactorial etiology which may complicate its diagnosis. The high accuracy performance of the proposed system with the current training dataset suggests that the proposed system would support the clinician’s decision by the help of using distinctive features from different domains.

Such a decision support system may also be helpful for the guidance and psychological counseling departments of high schools in addition to its possible use in psychiatry clinics. By using such a system, consultancy teachers in high schools can recognize students with a high risk for impulsivity and direct them to clinics on time. Thus, both students at high risk of impulsivity will be directed to clinics at the right time, and non-impulsive students will be prevented from creating crowdedness in clinics with incorrect predictions and/or preliminary diagnoses. The findings contribute to the development of an objective assessment of impulsivity and suggest the potential of fNIRS-derived biomarkers for the assessment of impulsivity.

7. REFERENCES

1. Stanford MS, Mathias CW, Dougherty DM, Lake SL, Anderson NE, Patton JH. Fifty years of the Barratt Impulsiveness Scale: An update and review. Vol. 47, Personality and Individual Differences. 2009. p. 385–95.
2. Daruna JH, Barnes PA. A neurodevelopmental view of impulsivity. The impulsive client: Theory, research, and treatment [Internet]. 2004 Oct 27 [cited 2022 Jun 2];23–37. Available from: /record/2004-14108-002
3. Patton JH, Stanford MS, Barratt ES. Factor structure of the barratt impulsiveness scale. Journal of Clinical Psychology. 1995 Nov;51(6):768–74.
4. Hoshi Y. Functional near-infrared spectroscopy: current status and future prospects. Journal of Biomedical Optics. 2007;12(6):062106.
5. Wylie GR, Graber HL, Voelbel GT, Kohl AD, DeLuca J, Pei Y, et al. Using co-variations in the Hb signal to detect visual activation: A near infrared spectroscopic imaging study. Neuroimage. 2009 Aug;47(2):473–81.
6. Quaresima V, Ferrari M. Functional Near-Infrared Spectroscopy (fNIRS) for Assessing Cerebral Cortex Function During Human Behavior in Natural/Social Situations: A Concise Review. Organizational Research Methods. 2019 Jan 18;22(1):46–68.
7. Jöbsis FF. Noninvasive, Infrared Monitoring of Cerebral and Myocardial Oxygen Sufficiency and Circulatory Parameters. Science (1979). 1977 Dec 23;198(4323):1264–7.
8. Abibullaev B, An J, Jin SH, Lee SH, Moon J il. Minimizing inter-subject variability in fNIRS-based brain–computer interfaces via multiple-kernel support vector learning. Medical Engineering & Physics. 2013 Dec 1;35(12):1811–8.
9. Faress A, Chau T. Towards a multimodal brain–computer interface: Combining fNIRS and fTCD measurements to enable higher classification accuracy. Neuroimage. 2013 Aug 15;77:186–94.
10. Coyle SM, Ward TE, Markham CM. Brain–computer interface using a simplified functional near-infrared spectroscopy system. Journal of Neural

Engineering [Internet]. 2007 Apr 27 [cited 2022 Jun 2];4(3):219. Available from: https://iopscience.iop.org/article/10.1088/1741-2560/4/3/007

11. Coyle S, Ward T, Markham C, McDarby G. On the suitability of near-infrared (NIR) systems for next-generation brain–computer interfaces. Physiological Measurement [Internet]. 2004 Jul 22 [cited 2022 Jun 2];25(4):815. Available from: https://iopscience.iop.org/article/10.1088/0967-3334/25/4/003

12. Kaiser V, Bauernfeind G, Kreilinger A, Kaufmann T, Kübler A, Neuper C, et al. Cortical effects of user training in a motor imagery based brain–computer interface measured by fNIRS and EEG. Neuroimage. 2014 Jan 15;85:432–44.

13. Bauernfeind G, Steyrl D, Brunner C, Muller-Putz GR. Single trial classification of fNIRS-based brain-computer interface mental arithmetic data: A comparison between different classifiers. In: 2014 36th Annual International Conference of the IEEE Engineering in Medicine and Biology Society. IEEE; 2014. p. 2004–7.

14. Pfurtscheller G, Allison BZ, Bauernfeind G, Brunner C, Solis Escalante T, Scherer R, et al. The hybrid BCI. Frontiers in Neuroscience. 2010;0:3.

15. Shin J, Müller KR, Hwang HJ. Near-infrared spectroscopy (NIRS)-based eyes-closed brain-computer interface (BCI) using prefrontal cortex activation due to mental arithmetic. Scientific Reports 2016 6:1 [Internet]. 2016 Nov 8 [cited 2022 Jun 2];6(1):1–11. Available from: https://www.nature.com/articles/srep36203

16. Schudlo LC, Chau T. Dynamic topographical pattern classification of multichannel prefrontal NIRS signals: II. Online differentiation of mental arithmetic and rest. Journal of Neural Engineering [Internet]. 2013 Dec 5 [cited 2022 Jun 2];11(1):016003. Available from: https://iopscience.iop.org/article/10.1088/1741-2560/11/1/016003

17. Naseer N, Qureshi NK, Noori FM, Hong KS. Analysis of Different Classification Techniques for Two-Class Functional Near-Infrared Spectroscopy-Based Brain-Computer Interface. Computational Intelligence and Neuroscience. 2016;2016.

18. Cubillo A, Halari R, Smith A, Taylor E, Rubia K. A review of fronto-striatal and fronto-cortical brain abnormalities in children and adults with Attention

Deficit Hyperactivity Disorder (ADHD) and new evidence for dysfunction in adults with ADHD during motivation and attention. Cortex. 2012 Feb 1;48(2):194–215.

19. Bledsoe JC, Xiao C, Chaovalitwongse A, Mehta S, Grabowski TJ, Semrud-Clikeman M, et al. Diagnostic Classification of ADHD Versus Control: Support Vector Machine Classification Using Brief Neuropsychological Assessment. Journal of Attention Disorders [Internet]. 2020 Sep 1 [cited 2022 Jun 2];24(11):1547–56. Available from: https://journals.sagepub.com/doi/10.1177/1087054716649666

20. Kim JW, Sharma V, Ryan ND. Predicting Methylphenidate Response in ADHD Using Machine Learning Approaches. International Journal of Neuropsychopharmacology [Internet]. 2015 Oct 1 [cited 2022 Jun 2];18(11):1–7. Available from: https://academic.oup.com/ijnp/article/18/11/pyv052/2910008

21. Monden Y, Dan I, Nagashima M, Dan H, Uga M, Ikeda T, et al. Individual classification of ADHD children by right prefrontal hemodynamic responses during a go/no-go task as assessed by fNIRS. NeuroImage: Clinical. 2015 Jan 1;9:1–12.

22. Ichikawa H, Kitazono J, Nagata K, Manda A, Shimamura K, Sakuta R, et al. Novel method to classify hemodynamic response obtained using multi-channel fNIRS measurements into two groups: Exploring the combinations of channels. Frontiers in Human Neuroscience. 2014 Jul 2;8(JULY):480.

23. Crippa A, Salvatore C, Molteni E, Mauri M, Salandi A, Trabattoni S, et al. The utility of a computerized algorithm based on a multi-domain profile of measures for the diagnosis of attention deficit/hyperactivity disorder. Frontiers in Psychiatry. 2017 Oct 3;8(OCT):189.

24. Wang XH, Jiao Y, Li L. Predicting clinical symptoms of attention deficit hyperactivity disorder based on temporal patterns between and within intrinsic connectivity networks. Neuroscience. 2017 Oct 24;362:60–9.

25. Uddin LQ, Kelly AMC, Biswal BB, Margulies DS, Shehzad Z, Shaw D, et al. Network homogeneity reveals decreased integrity of default-mode network in ADHD. Journal of Neuroscience Methods. 2008 Mar 30;169(1):249–54.

26. Orrù G, Pettersson-Yeo W, Marquand AF, Sartori G, Mechelli A. Using Support Vector Machine to identify imaging biomarkers of neurological and psychiatric disease: A critical review. Neuroscience & Biobehavioral Reviews. 2012 Apr 1;36(4):1140–52.
27. Peng H, Xia C, Wang Z, Zhu J, Zhang X, Sun S, et al. Multivariate Pattern Analysis of EEG-Based Functional Connectivity: A Study on the Identification of Depression. IEEE Access. 2019;7:92630–41.
28. Eysenck SBG, Eysenck HJ. The place of impulsiveness in a dimensional system of personality description. Br J Soc Clin Psychol [Internet]. 1977 [cited 2022 Jun 3];16(1):57–68. Available from: https://pubmed.ncbi.nlm.nih.gov/843784/
29. Ainslie G. Specious reward: a behavioral theory of impulsiveness and impulse control. Psychol Bull [Internet]. 1975 Jul [cited 2022 Jun 3];82(4):463–96. Available from: https://pubmed.ncbi.nlm.nih.gov/1099599/
30. Stroop JR. Studies of interference in serial verbal reactions. Journal of Experimental Psychology [Internet]. 1935 Dec [cited 2022 Jun 3];18(6):643–62. Available from: /record/1936-01863-001
31. MacLeod CM, Dunbar K. Training and Stroop-Like Interference: Evidence for a Continuum of Automaticity. Journal of Experimental Psychology: Learning, Memory, and Cognition. 1988;14(1):126–35.
32. Ivnik RJ, Malec JF, Smith GE, Tangalos EG, Petersen RC. Neuropsychological tests' norms above age 55: COWAT, BNT, MAE token, WRAT-R reading, AMNART, STROOP, TMT, and JLO. https://doi.org/101080/13854049608406689 [Internet]. 2007 [cited 2022 Jun 3];10(3):262–78. Available from: https://www.tandfonline.com/doi/abs/10.1080/13854049608406689
33. Jensen AR, Rohwer WD. The stroop color-word test: A review. Acta Psychologica. 1966 Jan 1;25(C):36–93.
34. Kane MJ, Engle RW. Working-Memory Capacity and the Control of Attention: The Contributions of Goal Neglect, Response Competition, and Task Set to Stroop Interference. Journal of Experimental Psychology: General. 2003 Mar;132(1):47–70.

35. Leung HC, Skudlarski P, Gatenby JC, Peterson BS, Gore JC. An event-related functional MRI study of the stroop color word interference task. Cereb Cortex [Internet]. 2000 [cited 2022 Jun 3];10(6):552–60. Available from: https://pubmed.ncbi.nlm.nih.gov/10859133/
36. Peterson BS, Skudlarski P, Gatenby JC, Zhang H, Anderson AW, Gore JC. An fMRI study of Stroop word-color interference: evidence for cingulate subregions subserving multiple distributed attentional systems. Biol Psychiatry [Internet]. 1999 May 15 [cited 2022 Jun 3];45(10):1237–58. Available from: https://pubmed.ncbi.nlm.nih.gov/10349031/
37. Pinti P, Tachtsidis I, Hamilton A, Hirsch J, Aichelburg C, Gilbert S, et al. The present and future use of functional near-infrared spectroscopy (fNIRS) for cognitive neuroscience. Ann N Y Acad Sci. 2020 Mar;1464(1):5–29.
38. Erdoğan SB, Yücel MA, Akin A. Analysis of task-evoked systemic interference in fNIRS measurements: Insights from fMRI. Neuroimage. 2014 Feb 15;87:490–504.
39. Akgül CB, Akin A, Sankur B. Extraction of cognitive activity-related waveforms from functional near-infrared spectroscopy signals. Medical and Biological Engineering and Computing 2006 44:11 [Internet]. 2006 Oct 24 [cited 2022 Jun 3];44(11):945–58. Available from: https://link.springer.com/article/10.1007/s11517-006-0116-3
40. Einalou Z, Maghooli K, Setarehdan SK, Akin A. Effective channels in classification and functional connectivity pattern of prefrontal cortex by functional near infrared spectroscopy signals. Optik (Stuttg). 2016 Mar 1;127(6):3271–5.
41. Dadgostar M, Setarehdan SK, Shahzadi S, Akin A. Functional connectivity of the PFC via partial correlation. Optik (Stuttg). 2016 Jun 1;127(11):4748–54.
42. Aydöre S, Mihçak MK, Çiftçi K, Akin A. On temporal connectivity of PFC via Gauss-Markov modeling of fNIRS signals. IEEE Transactions on Biomedical Engineering. 2010 Mar;57(3):761–8.
43. Chance B, Anday E, Nioka S, Zhou S, Hong L, Worden K, et al. A novel method for fast imaging of brain function, non-invasively, with light. Optics Express, Vol 2, Issue 10, pp 411-423 [Internet]. 1998 May 11 [cited 2022 Jun

3];2(10):411–23. Available from: https://opg.optica.org/viewmedia.cfm?uri=oe-2-10-411&seq=0&html=true

44. Zysset S, Müller K, Lohmann G, von Cramon DY. Color-word matching stroop task: separating interference and response conflict. Neuroimage [Internet]. 2001 [cited 2022 Jun 3];13(1):29–36. Available from: https://pubmed.ncbi.nlm.nih.gov/11133306/

45. Einalou Z, Maghooli K, Setarehdan SK, Akin A. Graph theoretical approach to functional connectivity in prefrontal cortex via fNIRS. https://doi.org/101117/1NPh44041407 [Internet]. 2017 Aug 21 [cited 2022 Jun 3];4(4):041407. Available from: https://www.spiedigitallibrary.org/journals/neurophotonics/volume-4/issue-4/041407/Graph-theoretical-approach-to-functional-connectivity-in-prefrontal-cortex-via/10.1117/1.NPh.4.4.041407.full

46. Strangman G, Culver JP, Thompson JH, Boas DA. A Quantitative Comparison of Simultaneous BOLD fMRI and NIRS Recordings during Functional Brain Activation. Neuroimage. 2002 Oct 1;17(2):719–31.

47. Watanabe A, Kato N, Kato T. Effects of creatine on mental fatigue and cerebral hemoglobin oxygenation. Neuroscience Research. 2002 Apr 1;42(4):279–85.

48. Dravida S, Adam J, Zhang NX, Hirsch J, Noah JA, Zhang X. Comparison of oxyhemoglobin and deoxyhemoglobin signal reliability with and without global mean removal for digit manipulation motor tasks. https://doi.org/101117/1NPh51011006 [Internet]. 2017 Sep 14 [cited 2022 Jun 3];5(1):011006. Available from: https://www.spiedigitallibrary.org/journals/neurophotonics/volume-5/issue-1/011006/Comparison-of-oxyhemoglobin-and-deoxyhemoglobin-signal-reliability-with-and-without/10.1117/1.NPh.5.1.011006.full

49. Plichta MM, Herrmann MJ, Baehne CG, Ehlis AC, Richter MM, Pauli P, et al. Event-related functional near-infrared spectroscopy (fNIRS): Are the measurements reliable? Neuroimage. 2006 May 15;31(1):116–24.

50. Cui X, Bray S, Bryant DM, Glover GH, Reiss AL. A quantitative comparison of NIRS and fMRI across multiple cognitive tasks. Neuroimage. 2011 Feb 14;54(4):2808–21.

51. Raichle ME, MacLeod AM, Snyder AZ, Powers WJ, Gusnard DA, Shulman GL. A default mode of brain function. Proc Natl Acad Sci U S A [Internet]. 2001 Jan 16 [cited 2022 Jun 3];98(2):676–82. Available from: www.pnas.org
52. Biswal B, Zerrin Yetkin F, Haughton VM, Hyde JS. Functional connectivity in the motor cortex of resting human brain using echo-planar MRI. Magn Reson Med [Internet]. 1995 [cited 2022 Jun 3];34(4):537–41. Available from: https://pubmed.ncbi.nlm.nih.gov/8524021/
53. Scarpina F, Tagini S. The stroop color and word test. Frontiers in Psychology. 2017 Apr 12;8(APR):557.
54. Akin A. Partial correlation-based functional connectivity analysis for functional near-infrared spectroscopy signals. https://doi.org/101117/1JBO2212126003 [Internet]. 2017 Dec 14 [cited 2022 Jun 3];22(12):126003. Available from: https://www.spiedigitallibrary.org/journals/journal-of-biomedical-optics/volume-22/issue-12/126003/Partial-correlation-based-functional-connectivity-analysis-for-functional-near-infrared/10.1117/1.JBO.22.12.126003.full
55. Firbank M, Okada E, Delpy DT. A Theoretical Study of the Signal Contribution of Regions of the Adult Head to Near-Infrared Spectroscopy Studies of Visual Evoked Responses. Neuroimage. 1998 Jul 1;8(1):69–78.
56. Latora V, Marchiori M. Efficient behavior of small-world networks. Phys Rev Lett [Internet]. 2001 Nov 5 [cited 2022 Jun 3];87(19):198701-1-198701–4. Available from: https://pubmed.ncbi.nlm.nih.gov/11690461/
57. Neubauer AC, Fink A. Intelligence and neural efficiency. Neuroscience & Biobehavioral Reviews. 2009 Jul 1;33(7):1004–23.
58. Fuster JM. The prefrontal cortex. The Prefrontal Cortex. 2015 Jul 31;1–444.
59. Prat CS, Keller TA, Just MA. Individual Differences in Sentence Comprehension: A Functional Magnetic Resonance Imaging Investigation of Syntactic and Lexical Processing Demands. Journal of Cognitive Neuroscience [Internet]. 2007 Dec 1 [cited 2022 Jun 3];19(12):1950–63. Available from: https://direct.mit.edu/jocn/article/19/12/1950/4375/Individual-Differences-in-Sentence-Comprehension-A

60. di Domenico SI, Rodrigo AH, Ayaz H, Fournier MA, Ruocco AC. Decision-making conflict and the neural efficiency hypothesis of intelligence: A functional near-infrared spectroscopy investigation. Neuroimage. 2015 Apr 1;109:307–17.
61. Liu Z, Wang L, Zhang Y, Chen CLP. A SVM controller for the stable walking of biped robots based on small sample sizes. Applied Soft Computing. 2016 Jan 1;38:738–53.
62. Lee SY, Lu RB, Wang LJ, Chang CH, Lu T, Wang TY, et al. Serum miRNA as a possible biomarker in the diagnosis of bipolar II disorder. Scientific Reports 2020 10:1 [Internet]. 2020 Jan 24 [cited 2022 Jun 5];10(1):1–10. Available from: https://www.nature.com/articles/s41598-020-58195-0
63. Hall M, Frank E, Holmes G, Pfahringer B, Reutemann P, Witten IH. The WEKA data mining software. ACM SIGKDD Explorations Newsletter [Internet]. 2009 Nov 16 [cited 2022 Jun 3];11(1):10–8. Available from: https://dl.acm.org/doi/abs/10.1145/1656274.1656278
64. Boser BE, Guyon IM, Vapnik VN. A training algorithm for optimal margin classifiers. In: Proceedings of the fifth annual workshop on Computational learning theory - COLT '92. New York, New York, USA: ACM Press; 1992. p. 144–52.
65. Platt JC. Sequential Minimal Optimization: A Fast Algorithm for Training Support Vector Machines [Internet]. 1998 [cited 2022 Jun 3]. Available from: https://www.microsoft.com/en-us/research/uploads/prod/1998/04/sequential-minimal-optimization.pdf
66. Hopfield JJ. Artificial Neural Networks. 1988.
67. Bebis G, Georgiopoulos M. Feed-forward neural networks. 1994.
68. Haykin S. Neural Networks: A Comprehensive Foundation (3rd Edition). The Knowledge Engineering Review [Internet]. 1999 [cited 2022 Jun 3];13(4):S0269888998214044. Available from: http://www.journals.cambridge.org/abstract_S0269888998214044
69. Rumelhart DE, McClelland JL. Learning Internal Representations by Error Propagation - MIT Press books. Parallel Distributed Processing: Explorations

in the Microstructure of Cognition: Foundations [Internet]. 1987 [cited 2022 Jun 3];318–62. Available from: https://ieeexplore.ieee.org/document/6302929

70. Erdoĝan SB, Özsarfati E, Dilek B, Kadak KS, Hanoĝlu L, Akin A. Classification of motor imagery and execution signals with population-level feature sets: implications for probe design in fNIRS based BCI. Journal of Neural Engineering [Internet]. 2019 Feb 19 [cited 2022 Jun 3];16(2):026029. Available from: https://iopscience.iop.org/article/10.1088/1741-2552/aafdca

71. Cui X, Bray S, Reiss AL. Speeded Near Infrared Spectroscopy (NIRS) Response Detection. PLOS ONE [Internet]. 2010 [cited 2022 Jun 3];5(11):e15474. Available from: https://journals.plos.org/plosone/article?id=10.1371/journal.pone.0015474

72. Hawkins DM, Basak SC, Mills D. Assessing Model Fit by Cross-Validation. Journal of Chemical Information and Computer Sciences [Internet]. 2003 Mar [cited 2022 Jun 3];43(2):579–86. Available from: https://pubs.acs.org/doi/abs/10.1021/ci025626i

73. Tai K, Chau T. Single-trial classification of NIRS signals during emotional induction tasks: Towards a corporeal machine interface. Journal of NeuroEngineering and Rehabilitation [Internet]. 2009 Nov 9 [cited 2022 Jun 3];6(1):1–14. Available from: https://jneuroengrehab.biomedcentral.com/articles/10.1186/1743-0003-6-39

74. Sitaram R, Zhang H, Guan C, Thulasidas M, Hoshi Y, Ishikawa A, et al. Temporal classification of multichannel near-infrared spectroscopy signals of motor imagery for developing a brain–computer interface. Neuroimage. 2007 Feb 15;34(4):1416–27.

75. Tanaka H, Katura T. Classification of change detection and change blindness from near-infrared spectroscopy signals. https://doi.org/101117/13606494 [Internet]. 2011 Aug 1 [cited 2022 Jun 3];16(8):087001. Available from: https://www.spiedigitallibrary.org/journals/journal-of-biomedical-optics/volume-16/issue-8/087001/Classification-of-change-detection-and-change-blindness-from-near-infrared/10.1117/1.3606494.full

76. Misawa T, Takano S, Shimokawa T, Hirobayashi S. A brain–computer interface for motor assist by the prefrontal cortex. Electronics and Communications in

Japan [Internet]. 2012 Oct 1 [cited 2022 Jun 3];95(10):1–8. Available from: https://onlinelibrary.wiley.com/doi/full/10.1002/ecj.11426

77. Keerthi SS, Shevade SK, Bhattacharyya C, Murthy KRK. Improvements to Platt's SMO Algorithm for SVM Classifier Design. Neural Computation [Internet]. 2001 Mar 1 [cited 2022 Jun 3];13(3):637–49. Available from: https://direct.mit.edu/neco/article/13/3/637/6485/Improvements-to-Platt-s-SMO-Algorithm-for-SVM

78. Zhu CZ, Zang YF, Cao QJ, Yan CG, He Y, Jiang TZ, et al. Fisher discriminative analysis of resting-state brain function for attention-deficit/hyperactivity disorder. Neuroimage. 2008 Mar 1;40(1):110–20.

79. Colby JB, Rudie JD, Brown JA, Douglas PK, Cohen MS, Shehzad Z. Insights into multimodal imaging classification of ADHD. Frontiers in Systems Neuroscience. 2012 Aug 16;0(AUG 2012):1–18.

80. Lim LG, Ung WC, Chan YL, Lu CK, Funane T, Kiguchi M, et al. Optimizing mental workload estimation by detecting baseline state using vector phase analysis approach. IEEE Transactions on Neural Systems and Rehabilitation Engineering. 2021;29:597–606.

81. Preti MG, Bolton TA, van de Ville D. The dynamic functional connectome: State-of-the-art and perspectives. Neuroimage. 2017 Oct 15;160:41–54.

82. Muthukrishnan R, Rohini R. LASSO: A feature selection technique in predictive modeling for machine learning. 2016 IEEE International Conference on Advances in Computer Applications, ICACA 2016. 2017 Mar 27;18–20.

83. Al-shargie F, Boon Tang T, Kiguchi M, Bishop S, Duncan J, Brett M, et al. Assessment of mental stress effects on prefrontal cortical activities using canonical correlation analysis: an fNIRS-EEG study. Biomedical Optics Express, Vol 8, Issue 5, pp 2583-2598 [Internet]. 2017 May 1 [cited 2022 Jun 3];8(5):2583–98. Available from: https://opg.optica.org/viewmedia.cfm?uri=boe-8-5-2583&seq=0&html=true

84. Al-shargie F, Kiguchi M, Badruddin N, Dass SC, Fadzil Mohammad Hani A, Boon Tang T, et al. Mental stress assessment using simultaneous measurement of EEG and fNIRS. Biomedical Optics Express, Vol 7, Issue 10, pp 3882-3898

[Internet]. 2016 Oct 1 [cited 2022 Jun 3];7(10):3882–98. Available from: https://opg.optica.org/viewmedia.cfm?uri=boe-7-10-3882&seq=0&html=true

85. Hoshi Y. Functional near-infrared optical imaging: Utility and limitations in human brain mapping. Psychophysiology [Internet]. 2003 Jul 1 [cited 2022 Jun 3];40(4):511–20. Available from: https://onlinelibrary.wiley.com/doi/full/10.1111/1469-8986.00053

86. Hoshi Y, Kobayashi N, Tamura M. Interpretation of near-infrared spectroscopy signals: A study with a newly developed perfused rat brain model. Journal of Applied Physiology [Internet]. 2001 [cited 2022 Jun 3];90(5):1657–62. Available from: https://journals.physiology.org/doi/full/10.1152/jappl.2001.90.5.1657

87. Dresler T, Ehlis AC, Plichta MM, Richter MM, Jabs B, Lesch KP, et al. Panic disorder and a possible treatment approach by means of high-frequency rTMS: A case report. http://dx.doi.org/101080/15622970902898147 [Internet]. 2009 [cited 2022 Jun 3];10(4 PART 3):991–7. Available from: https://www.tandfonline.com/doi/abs/10.1080/15622970902898147